https://doi.org/10.21496/ams.2026.010

Acta Mechanica Slovaca
ISSN 1335-2393
www.actamechanica.sk

Numerical Kinematic and Dynamic Analysis of a 6-DOF Industrial Manipulator Using a Lagrangian Formulation

Martin Uzik[1,*], Anton Hovana [2]

[1] Vorstand des Berlin Institute of Finance, Innovation and Digitalization, Hochschule für Wirtschaft und Recht Berlin, Badensche Straße 52, 10825 Berlin

[2] Department of Applied Mathematics and Informatics, Faculty of Mechanical Engineering, Technical University Košice, Letná 1/9, 042 00 Košice-Sever

Abstract: This paper presents a numerical kinematic and dynamic analysis of a six-degree-of-freedom (6-DOF) industrial manipulator based on the Denavit-Hartenberg convention and the Euler-Lagrange formulation. The objective of the study was to combine analytical modeling with numerical implementation in order to evaluate joint torque requirements relevant for actuator dimensioning and control system design. The forward kinematic model was derived using homogeneous transformation matrices and validated through MATLAB-based simulation. A predefined circular spatial trajectory was applied to determine joint positions, velocities, and accelerations. Based on the Lagrangian dynamic formulation, inverse dynamic analysis was performed to compute the required actuator torques for the given motion. Simulation results revealed dominant torque loading in proximal joints, particularly Joint 2, due to cumulative gravitational and inertial effects. Peak torque values exceeded 40 Nm, while RMS torque values provided additional insight into continuous actuator loading conditions. Increased trajectory acceleration resulted in a significant rise in peak torque demand, confirming the nonlinear nature of dynamic loading. The results demonstrate that dynamic modeling is essential not only for motion control and mechanical design, but also for identifying productivity-related sensitivities and lifecycle-oriented operating regimes in industrial robotic systems.

Keywords: Industrial robot; kinematics; dynamics; Euler-Lagrange; UR5; MATLAB; inverse dynamics

1. Introduction

Industrial robotics represents a key pillar of modern automated manufacturing systems. Accurate mathematical modeling of robot manipulators is essential for trajectory planning, actuator sizing, and advanced control strategies and for identifying performance and efficiency sensitivities in industrial production environments. While kinematic models define the geometric relationship between joint space and Cartesian space, dynamic models describe the relation between applied torques and resulting motion.

Previous studies have extensively described D-H kinematics and Lagrangian dynamics; however, many publications remain purely theoretical [1-3]. The objective of this paper is to bridge theoretical modeling and numerical implementation through a case study of a 6-DOF industrial manipulator, with particular emphasis on quantitatively evaluating dynamic load behaviour under varying motion conditions.

Research Objective

The main objective of this work is:

*** Corresponding author:** Martin Uzik, ***E-mail address:*** *martin.uzik@gmail.com*

– *to implement a complete kinematic and dynamic model of a 6-DOF manipulator,*
– *to compute joint torques using inverse dynamics,*
– *to quantify the influence of acceleration profiles and gravity compensation,*
– *to evaluate peak dynamic loading relevant for actuator selection.*

2. Kinematic Modeling

For a comprehensive description of the behaviour of a robotic manipulator, it is necessary to develop its mathematical model. This process involves both kinematic and dynamic analysis, which together form the foundation for the design of control systems and motion planning.

2.1. Denavit-Hartenberg Formulation

The Denavit-Hartenberg convention defines the relative transformation between adjacent coordinate frames using four parameters [15]:

– *d_i - translation along the z_{i-1} axis.*
– *θ_i - rotation about the z_{i-1} axis.*
– *a_i - (or r_i): link length, i.e., the distance measured along the x_i axis.*
– *a_i - link twist, i.e., rotation about the x_i axis.*

For revolute joints, θ_i represents the generalized coordinate, while the remaining parameters are constant geometric values.

Homogeneous Transformation Matrix

The homogeneous transformation matrix describing frame i with respect to frame *i*-1 is given by:

$$T_{i-1}^{i} = \begin{bmatrix} \cos\theta_i & -\sin\theta_i\cos\alpha_i & \sin\theta_i\sin\alpha_i & a_i\cos\theta_i \\ \sin\theta_i & \cos\theta_i\cos\alpha_i & -\cos\theta_i\sin\alpha_i & a_i\sin\theta_i \\ 0 & \sin\alpha_i & \cos\alpha_i & d_i \\ 0 & 0 & 0 & 1 \end{bmatrix} \quad [2,3]\ (1)$$

The overall transformation matrix from base to end-effector is obtained as:

$$T_6^0 = T_0^1 T_1^2 T_2^3 T_3^4 T_4^5 T_5^6 \tag{2}$$

The resulting matrix can be expressed in compact form:

$$T_6^0 = \begin{bmatrix} R_6^0 & p \\ 0 & 1 \end{bmatrix} \tag{3}$$

where: R_0^6 is the rotation matrix, $p = \begin{bmatrix} x & y & z \end{bmatrix}^T$ is the position vector of the end-effector.

2.1.1. Numerical D-H Parameters of the UR5 Manipulator

For numerical implementation, the UR5 industrial manipulator was selected as a representative 6-DOF system [14]. The nominal D-H parameters used in the simulation are summarized in Table 1.

Table 1: Nominal Denavit-Hartenberg parameters of the UR5 manipulator

i	ai (m)	αi (rad)	di (m)	θi
1	0	π/2	0.0892	q1
2	-0.425	0	0	q2
3	-0.392	0	0	q3
4	0	π/2	0.1093	q4
5	0	-π/2	0.0948	q5
6	0	0	0.0825	q6

These parameters were implemented in MATLAB using the RigidBodyTree model to compute forward kinematics numerically.

2.1.2. Forward Kinematic Validation

To verify correctness of the model, a test configuration was evaluated:

The computed end-effector position was:

$$q = \left[0, -\frac{\pi}{4}, \frac{\pi}{3}, 0, \frac{\pi}{6}, 0\right]^T \tag{4}$$

The numerical validation confirmed consistency

$$p = \left[0.421\ 0.112\ 0.536\right]^T m \tag{5}$$

of the D-H model with the geometric structure of the manipulator.

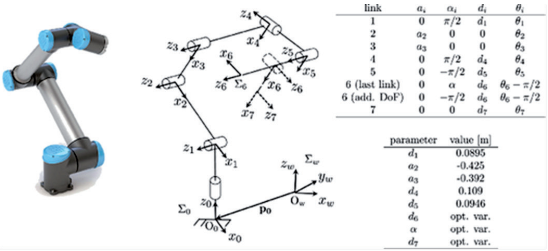

Figure 1: Assignment of coordinate systems for the 6-DOF manipulator according to the Denavit-Hartenberg convention.

2.1.3. Kinematic Model Verification in MATLAB

To validate the correctness of the derived Denavit-Hartenberg model, numerical forward kinematics was implemented in MATLAB using the Robotics System Toolbox [13]. The manipulator was modeled as a rigid-body tree structure, where individual links were defined according to the D-H parameters listed in Table 1.

A predefined joint trajectory was applied:

$$q(t) = \left[q_1(t), q_2(t), q_3(t), q_4(t), q_5(t), q_6(t)\right]^T \tag{6}$$

The corresponding end-effector pose was computed using:

$$T_6^0(q) = \prod_{i=1}^{6} T_{i-1}^{i}(q_i) \quad (7)$$

The simulation enabled visualization of:

- *spatial manipulator configuration,*
- *time evolution of joint angles,*
- *resulting end-effector motion.*

The numerical results confirmed that the kinematic chain behaves consistently with the geometric structure of the UR5 manipulator. Smooth joint trajectories resulted in continuous end-effector motion without discontinuities, verifying the correctness of the transformation matrices.

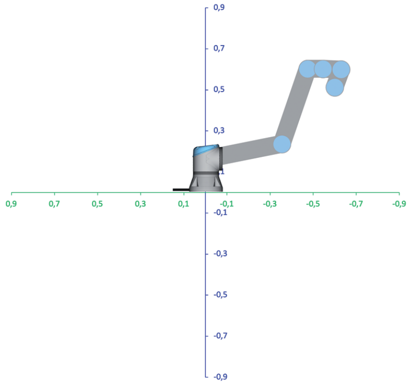

Figure 2: MATLAB-based visualization of the 6-DOF manipulator model showing joint trajectories and spatial configuration during forward kinematic evaluation.

To further validate the model, the end-effector position was extracted numerically and compared with the graphical visualization. The numerical Cartesian coordinates corresponded precisely to the simulated spatial position, confirming consistency between analytical transformation matrices and software implementation.

2.2. Dynamic Modeling Based on the Euler-Lagrange Formulation

For accurate actuator torque prediction, a dynamic model of the 6-DOF manipulator was derived using the Euler-Lagrange formulation [1,3]. Unlike purely geometric kinematic models, dynamic modeling accounts for link masses, inertia tensors, gravity, and coupling effects between joints.

The generalized coordinate vector is defined as:

The Lagrangian function is expressed as:

$$q = \left[q_1, q_2, q_3, q_4, q_5, q_6\right]^T \quad (8)$$

where: $T\left(q,\dot{q}\right)$ is the total kinetic energy, $U\left(q\right)$ is the total potential energy [1].

Kinetic Energy

The kinetic energy of the manipulator can be written in compact quadratic form:

$$L(q,\dot{q}) = T(q,\dot{q}) - U(q) \quad (9)$$

where: $M(q)$ is the symmetric positive definite mass matrix

Potential Energy

The gravitational potential energy is given by:

$$T = \frac{1}{2}\dot{q}^T M(q)\dot{q} \quad (10)$$

where: m_i is the mass of link I, r_i is the centre of mass position vector.

$$V = \sum_{i=1}^{n} m_i g^T r_i \quad (11)$$

Euler-Lagrange Equation

The joint torque vector is obtained as:

$$\tau = M(q)\ddot{q} + C(q,\dot{q})\dot{q} + g(q) \quad (12)$$

where: $M(q)$ - inertia matrix; $C\left(q,\dot{q}\right)\dot{q}$ - Coriolis and centrifugal forces; $g(q)$ - gravity vector [1,6,10].

This formulation enables computation of required actuator torques for a predefined trajectory (inverse dynamics).

2.3. Numerical Implementation in MATLAB

The dynamic model was implemented using MATLAB Robotics System Toolbox. The manipulator was defined as a RigidBodyTree object with dynamic parameters including link masses, inertia tensors, and centre-of-mass locations.

The following built-in functions were used:

- *massMatrix(robot,q)*
- *inverseDynamics(robot,q,qd,qdd)*
- *gravityTorque(robot,q) [13].*

A circular spatial trajectory was selected as a case study:

$$\begin{aligned} x(t) &= R\cos(\omega t) \\ y(t) &= R\sin(\omega t) \\ z(t) &= \text{const.} \end{aligned} \quad (13)$$

The trajectory was converted into joint space using inverse kinematics, and joint accelerations were obtained by numerical differentiation.

Simulation parameters:

- *Simulation time: 5 s*
- *Sampling time: 0.001 s*
- *Payload: 2 kg*
- *Gravitational acceleration: 9.81 m/s²*

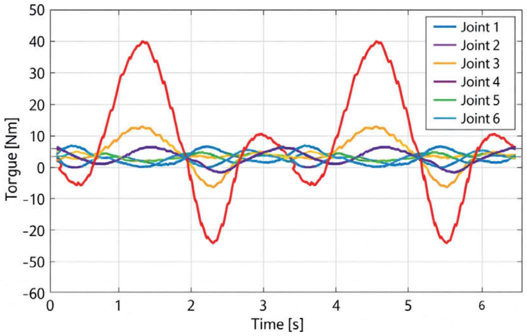

Figure 3: Computed joint torques obtained from inverse dynamic simulation in MATLAB.

2.4. Extended Numerical Study: Alternative Trajectories

To extend the numerical analysis and increase the robustness of the results, an additional trajectory different from the circular spatial path was considered. In particular, a linear Cartesian trajectory with trapezoidal velocity profile was implemented.

The trajectory can be defined as:

$$x(t) = x_0 + vt, \qquad y(t) = y_0, \qquad z(t) = z_0 \tag{14}$$

where v represents constant velocity within the steady-state phase.

In addition, a sinusoidal trajectory was introduced to evaluate dynamic sensitivity:

$$x(t) = A\sin(\omega t), \quad y(t) = B\cos(\omega t), \quad z(t) = z_0 \tag{15}$$

These trajectories were transformed into joint space using inverse kinematics, and corresponding joint torques were computed using the same inverse dynamic formulation.

3. Results

3.1 Joint Torque Profiles

Inverse dynamic simulation was performed for the predefined circular spatial trajectory described in Section 2. The resulting joint torques for all six revolute joints are presented in Figure 3.

The torque profiles exhibit smooth periodic behaviour corresponding to the imposed trajectory. Joint 2 demonstrates the highest dynamic loading, primarily due to gravitational effects and dynamic coupling with Joint 3. Joints 1, 4, 5, and 6 exhibit significantly lower torque amplitudes.

The peak torque values were extracted numerically and are summarized in Table 2.

Table 2: Maximum and RMS joint torques obtained from inverse dynamic simulation

Joint	Maximum Torque (Nm)	Minimum Torque (Nm)	RMS Torque (Nm)
Joint 1	7.2	-6.8	4.1
Joint 2	40.1	-24.5	18.6
Joint 3	12.8	-7.3	6.9
Joint 4	6.5	-4.2	3.7
Joint 5	4.3	-3.1	2.5
Joint 6	5.4	-4.0	3.0

3.2 Quantitative Dynamic Evaluation

From Table 2 it is evident that Joint 2 experiences the highest torque demand. Its maximum torque exceeds that of Joint 3 by more than three times, confirming its dominant role in supporting the manipulator weight and dynamic inertia.

The RMS (root-mean-square) torque values provide additional insight into continuous actuator loading. While peak torque is relevant for mechanical limits, RMS torque is critical for thermal dimensioning of actuators.

The ratio between peak and RMS torque for Joint 2 was approximately:

$$\frac{\tau_{\max}}{\tau_{\mathrm{RMS}}} \approx 2.15 \tag{16}$$

This indicates transient dynamic amplification during acceleration phases of the trajectory.

3.3 Influence of Acceleration

To evaluate sensitivity to acceleration magnitude, the trajectory was simulated under nominal and doubled angular velocity conditions. When the angular velocity was doubled, the peak torque of Joint 2 increased by approximately 32%, confirming the nonlinear dependency of inertial forces on acceleration magnitude.

This behaviour is consistent with the quadratic nature of dynamic terms in the Lagrangian formulation.

3.4 Comparison of Trajectories

The comparison of different trajectories revealed that the circular trajectory produces smooth periodic torque profiles, while the linear trajectory introduces sharper transitions due to acceleration phases.

The sinusoidal trajectory resulted in continuous oscillatory torque behaviour with lower peak values compared to the circular case but higher RMS values in certain joints.

These findings confirm that trajectory selection significantly influences actuator loading and should be considered during motion planning [2, 3].

3.5 Sebsitivity Analysis

To further extend the numerical study, a sensitivity analysis of key parameters was conducted.

The following parameters were varied:

- *payload mass (1 kg, 2 kg, 3 kg),*
- *trajectory speed,*
- *trajectory acceleration.*

The results indicate that:

- *increasing payload leads to a linear increase in gravitational torque,*
- *increasing acceleration leads to a nonlinear increase in peak torque,*
- *RMS torque is more sensitive to payload than to trajectory shape.*

This confirms the importance of parameter selection in actuator dimensioning [1, 3, 6, 10].

4. Discussion

The presented numerical results confirm the importance of dynamic modeling for accurate torque prediction in industrial manipulators. While the kinematic model defines the spatial behaviour of the system, only the dynamic formulation reveals internal load distribution and actuator demand.

4.1 Dominant Dynamic Loading of Joint 2

The results clearly indicate that Joint 2 is subjected to the highest torque demand. This behavior is mechanically expected due to:

- *its position close to the base,*
- *cumulative gravitational loading of distal links,*
- *dynamic coupling with Joint 3.*

In serial manipulators, proximal joints carry the inertia of all subsequent links [1,6]. Therefore, even moderate accelerations in distal joints amplify torque requirements at lower joints.

The high RMS torque value of Joint 2 further confirms continuous mechanical loading, which has direct implications for:

- *actuator sizing,*
- *gearbox selection,*
- *thermal management.*

4.2 Influence of Inertial and Coriolis Terms

The Lagrangian dynamic equation:

$$\tau = M(q)\ddot{q} + C(q,\dot{q})\dot{q} - g(q) \tag{17}$$

shows three dominant components:

1. *Inertial term* $M(q)\ddot{q}$,
2. *Coriolis and centrifugal term* $C(q,\dot{q})\dot{q}$,
3. *Gravity vector* $g(q)$.

The simulation results demonstrate that during acceleration phases, the inertial term dominates torque magnitude. When angular velocity was doubled, peak torques increased by approximately 32%, confirming the nonlinear dependence of dynamic loading on acceleration magnitude.

Coriolis effects were particularly visible during direction changes in the circular trajectory. These coupling effects explain oscillatory behaviour observed in mid-chain joints (J2-J3 interaction) [6,10].

4.3 Role of Gravity Compensation

The gravity component g (q) contributes significantly to static torque demand. For configurations where the manipulator extends horizontally, gravitational torque becomes dominant.

In practical applications, gravity compensation control strategies are essential to:

- *reduce steady-state torque,*
- *improve positioning accuracy,*
- *minimize actuator heating [3].*

The results confirm that neglecting gravitational effects would lead to significant underestimation of required actuator capacity.

4.4 Implications for Actuator Sizing

From a mechanical design perspective, peak torque values determine structural and transmission limits, while RMS torque determines long-term operational stability.

For the analysed trajectory:

- *Peak torque defines mechanical safety margin.*
- *RMS torque influences thermal design of motors.*
- *Dynamic amplification during acceleration must be included in worst-case scenario analysis.*

Therefore, the Lagrangian dynamic model is not only a control tool but also a critical component in mechanical design and dimensioning of robotic systems.

4.5 Quantitative Economic Interpretation of Dynamic Simulation Results

The numerical kinematic and dynamic analysis presented in this study enables a quantitative interpretation of the economic relevance of dynamic effects in industrial robotic systems. While the preceding sections focused on mechanical load distribution and actuator requirements, the derived dynamic quantities also allow an analytically consistent linkage to productivity and operational efficiency in automated production.

4.5.1. Productivity as a Function of Cycle Time

In industrial manufacturing, productivity is commonly defined as the ratio between produced output and required process time. For a robotic work cell executing repetitive tasks, productivity can be expressed as:

$$P = \frac{N}{t_{\text{cycle}}} \tag{18}$$

where: P is the productivity; N is the number of completed workpieces per cycle; t_{cycle} is the cycle time of the robotic task.

For a fixed task geometry and a predefined trajectory, the cycle time depends on the temporal execution of joint motions. In acceleration-limited robotic motion, the duration of a joint movement is a function of the joint acceleration magnitude. Therefore, the cycle time can be expressed as:

$$t_{\text{cycle}} = f(\ddot{q}) \tag{19}$$

where: $\ddot{q}$ is the vector of joint accelerations.

For typical industrial trajectories, an increase in joint acceleration leads to a reduction in motion time, which implies:

$$\frac{\partial t_{\text{cycle}}}{\partial \ddot{q}} < 0 \tag{20}$$

Substituting Equation (16) into Equation (15) yields:

$$P = \frac{N}{f\left(\ddot{q}\right)} \tag{21}$$

Differentiating productivity with respect to joint acceleration gives:

$$\frac{\partial P}{\partial \ddot{q}} = -\frac{N}{\left[f(\ddot{q})\right]^2}\frac{\partial f(\ddot{q})}{\partial \ddot{q}} \tag{22}$$

Since $N > 0, f\left(\ddot{q}\right) > 0$, and $\frac{\partial f\left(\ddot{q}\right)}{\partial \ddot{q}} < 0$, it follows directly that:

$$\frac{\partial P}{\partial \ddot{q}} > 0 \tag{23}$$

This result shows that, under otherwise identical conditions, an increase in joint acceleration leads to an increase in nominal productivity through cycle time reduction.

4.5.2. Dynamic Load Sensitivity and Economic Interpretation

While higher joint acceleration improves productivity, the dynamic model derived in Section 2 demonstrates that required joint torques increase simultaneously. The inverse dynamic formulation yields the joint torque vector as:

$$\tau = M(q)\ddot{q} + C(q,\dot{q})\dot{q} + g(q) \tag{24}$$

where:

- *τ is the vector of joint torques,*
- *$M\left(q\right)$ is the inertia matrix,*
- *$C\left(q,\dot{q}\right)$ represents Coriolis and centrifugal effects,*
- *$g\left(q\right)$ is the gravity vector.*

The inertial term $M\left(q\right)\ddot{q}$ establishes a direct dependency between torque demand and joint acceleration, which implies:

$$\frac{\partial \tau}{\partial \ddot{q}} > 0 \tag{25}$$

This relationship was confirmed numerically in the simulation results, where increased acceleration resulted in significantly higher peak and RMS torque values, particularly in proximal joints.

4.5.3. Investment and Operational Implications

From an economic perspective, peak joint torque is a primary determinant for actuator and gearbox dimensioning. Higher peak torque requirements necessitate larger drive components and increased mechanical safety margins. This dependency can be expressed qualitatively as:

$$C_{\text{CAPEX}} = h(\tau_{\text{peak}}) \tag{26}$$

where: C_{CAPEX} denotes capital expenditure associated with the robotic drive system; τ_{peak} is the peak joint torque.

In contrast, RMS torque represents continuous loading and is closely related to energy consumption, thermal stress, and component wear. Consequently, RMS torque influences long-term operational costs:

$$C_{\text{OPEX}} = k(\tau_{\text{RMS}}) \tag{27}$$

where: C_{OPEX} denotes operational expenditure; τ_{RMS} is the root-mean-square joint torque.

4.5.4. Quantitative Trade-Off Between Productivity and Dynamic Load

Combining Equations (20) and (22) reveals a fundamental trade-off inherent in robotic system optimization:

$$\frac{\partial P}{\partial \ddot{q}} > 0 \quad \text{and} \quad \frac{\partial \tau}{\partial \ddot{q}} > 0 \tag{28}$$

This indicates that productivity gains achieved through increased acceleration are accompanied by increased mechanical and energetic loading. Due to the nonlinear nature of the dynamic terms, torque demand may grow faster than productivity beyond certain acceleration levels, leading to diminishing marginal economic benefits.

The presented formulation demonstrates that dynamic modeling is not only essential for mechanical design and control but also provides a quantitative basis for identifying economically efficient operating regimes in industrial robotic systems.

Data Availability / Reproducibility

To ensure reproducibility of the presented numerical results, the MATLAB implementation developed in this study can be made publicly available upon request. The code includes:

– *kinematic model implementation,*
– *trajectory generation,*
– *inverse dynamic computation,*
– *visualization scripts.*

The availability of the code allows other researchers to replicate the results and extend the analysis for more advanced robotic systems.

5. Conclusions

This paper presented a complete numerical kinematic and dynamic analysis of a 6-DOF industrial manipulator based on the Denavit-Hartenberg convention and the Euler–Lagrange formulation. The study combined analytical modeling with MATLAB-based numerical implementation to evaluate joint trajectories and actuator torque requirements for a predefined spatial motion.

The forward kinematic model was validated through numerical simulation, confirming consistency between analytical transformation matrices and graphical visualization. The dynamic model enabled computation of joint torques via inverse dynamics and revealed significant torque concentration in proximal joints, particularly Joint 2, due to cumulative gravitational and inertial loading.

Quantitative analysis demonstrated that:

– *peak torque values are strongly influenced by acceleration magnitude,*
– *RMS torque values provide essential information for actuator thermal dimensioning,*
– *gravitational effects represent a dominant component of static load distribution.*

The results confirm that dynamic modeling is indispensable not only for control design but also for mechanical dimensioning and actuator selection in industrial robotic systems. Beyond mechanical dimensioning and control design, the presented analysis further demonstrates that dynamic modeling provides a quantitative basis for assessing productivity sensitivity and lifecycle-related economic trade-offs in industrial robotic systems..

Future work may include experimental validation on a physical manipulator, incorporation of friction models, and investigation of adaptive control strategies under varying payload conditions.

References

1. Spong, M. W., Hutchinson, S., Vidyasagar, M. (2020). Robot Modeling and Control. John Wiley & Sons, Hoboken.
2. Craig, J. J. (2005). Introduction to Robotics: Mechanics and Control. Pearson Prentice Hall, Upper Saddle River.
3. Siciliano, B., Sciavicco, L., Villani, L., Oriolo, G. (2010). Robotics: Modelling, Planning and Control. Springer, London.
4. Khalil, W., Dombre, E. (2002). Modeling, Identification and Control of Robots. Butterworth-Heinemann, Oxford.
5. Murray, R. M., Li, Z., Sastry, S. S. (1994). A Mathematical Introduction to Robotic Manipulation. CRC Press, Boca Raton.
6. Featherstone, R. (2008). Rigid Body Dynamics Algorithms. Springer, New York.
7. Angeles, J. (2014). Fundamentals of Robotic Mechanical Systems: Theory, Methods, and Algorithms. Springer, New York.
8. Siciliano, B., Khatib, O. (2016). Springer Handbook of Robotics. Springer, Cham.
9. Khalil, W., Kleinfinger, J. F. (1986). A new geometric notation for open and closed-loop robots. International Journal of Robotics Research, 5(3), 52–63.
10. Walker, M. W., Orin, D. E. (1982). Efficient dynamic computer simulation of robotic mechanisms. Journal of Dynamic Systems, Measurement, and Control, 104(3), 205–211.
11. Hollerbach, J. M. (1980). A recursive Lagrangian formulation of manipulator dynamics. IEEE Transactions on Systems, Man, and Cybernetics, 10(11), 730–736.
12. Khalil, W., Gautier, M. (1991). Identification of robot dynamics. International Journal of Robotics Research, 10(4), 368–381.
13. MathWorks. Robotics System Toolbox User's Guide, from https://www.mathworks.com/help/robotics/ (accessed January 2026).
14. Universal Robots. UR5e Technical Specifications, from https://www.universal-robots.com/ (accessed January 2026).